Available online at www.sciencedirect.com
SCIENCE DIRECT®
Biochemical Pharmacology 66 (2003) 2201–2212
Biochemical Pharmacology
www.elsevier.com/locate/biochempharm

Inhibition of heme crystal growth by antimalarials and other compounds: implications for drug discovery

Curtis Robert Chong[a], David Joseph Sullivan Jr.[b,*]

[a]*Department of Pharmacology, Medical Scientist Training Program, The Johns Hopkins University School of Medicine, 725 North Wolfe Street, Baltimore, MD 21205, USA*
[b]*W. Harry Feinstone Department of Molecular Microbiology and Immunology, The Malaria Research Institute, Bloomberg School of Public Health, The Johns Hopkins University, 615 North Wolfe St. Baltimore, MD 21205, USA*

Received 10 April 2003; accepted 18 August 2003

Abstract

During intraerythrocytic infection, *Plasmodium falciparum* parasites crystallize toxic heme released during hemoglobin catabolism. The proposed mechanism of quinoline inhibition of crystal growth is either by a surface binding or a substrate sequestration mechanism. The kinetics of heme crystal growth was examined in this work using a new high-throughput crystal growth determination assay based on the differential solubility of free vs. crystalline FP in basic solutions. Chloroquine ($IC_{50} = 4.3$ μM) and quinidine ($IC_{50} = 1.5$ μM) showed a previously not recognized reversible inhibition of FP crystal growth. This inhibition decreased by increasing amounts of heme crystal seed, but not by greater amounts of FP substrate. Crystal growth decreases as pH rises from 4.0 to 6.0, except for a partial local maxima reversal from pH 5.0 to 5.5 that coincides with increased FP solubility. The new crystal growth determination assay enabled a partial screen of existing clinical drugs. Nitrogen heterocycle cytochrome P450 inhibitors also reversibly blocked FP crystal growth, including the azole antifungal drugs clotrimazole ($IC_{50} = 12.9$ μM), econazole ($IC_{50} = 19.7$ μM), ketoconazole ($IC_{50} = 6.5$ μM), and miconazole ($IC_{50} = 21.4$ μM). Fluconazole did not inhibit. Both subcellular fractionation of parasites treated with subinhibitory concentrations of ketoconazole and *in vitro* hemozoin growth assays demonstrated copurification of hemozoin and ketoconazole. The chemical diversity of existing CYP inhibitor libraries that bind FP presents new opportunities for the discovery of antimalarial drugs that block FP crystal growth by a surface binding mechanism and possibly interfere with other FP-sensitive *Plasmodium* pathways.

Keywords: Hemozoin; Chloroquine; Heme crystal; Ketoconazole; Quinidine; Malaria; *Plasmodium falciparum*

1. Introduction

The emergence of drug-resistant *Plasmodium falciparum* parasites makes antimalarial development a global public health priority [1]. Each year malaria causes an estimated 1.5–2.7 million deaths and affects some 300–500 million people worldwide [2,3]. Several approaches to develop new antimalarials include natural product screens, *de novo* drug design, chemical modification of existing antimalarials, and screening drugs currently in clinical use to treat other diseases [4–6].

One of the main targets of antimalarial action is the process of hemoglobin heme or iron-protoporphyrin IX (FP) detoxification by *P. falciparum*. During intraerythrocytic infection, up to 75% of host hemoglobin at a concentration of 5 mM is catabolized in the acidic parasite food vacuole [7,8]. The almost molar amounts of soluble FP released from this process potentially inhibits parasite proteases, mediates free radical reactions, and damages membranes [9,10]. In the absence of a heme oxygenase activity to detoxify FP, parasites crystallize oxidized FP into an insoluble, inert crystal called hemozoin. The hemozoin crystal is composed of unit cells of FP dimers (also known as Fe1–O41 dimers) coordinated by reciprocal iron to side chain carboxylate bonds [11]. The individual head to tail dimers form a hydrogen bond network to form the biocrystals [12]. Hemozoin from *Plasmodium*

* Corresponding author. Tel.: +1-410-614-1562; fax: +1-410-955-0105.
E-mail address: dsulliva@jhsph.edu (D.J. Sullivan Jr.).
Abbreviations: FP, iron-protoporphyrin IX or heme; ICG, inhibition of crystal growth; CYP, cytochrome P450.

0006-2952/$ – see front matter © 2003 Elsevier Inc. All rights reserved.
doi:10.1016/j.bcp.2003.08.009

parasites is structurally identical to synthetic β-hematin (Fe^{III}-protoporphyrin IX)$_2$, which can be prepared by incubating FP in acetic acid solutions at high temperature or under base abstraction in anhydrous conditions [11,13–15]. Appreciable crystal growth under physiologic temperature, pH, acid concentration and FP conditions within 24 hr *in vitro* has been nucleated by *Plasmodium* histidine-rich proteins [16,17], lipids [18,19], and pre-existing hemozoin or β-hematin [20–22].

Quinoline antimalarial drugs such as chloroquine and quinidine act by inhibiting FP crystal growth [23]. Inhibition is stage-specific for parasites actively degrading FP [24], and the quinolines concentrate to millimolar levels in the digestive vacuole, despite circulating in the plasma at nanomolar concentrations [25,26]. Numerous studies have shown that the quinolines bind FP noncovalently [27–31]. An additional theory suggests the FP–quinoline complex incorporates into a growing crystal face that blocks further crystal growth defined here as addition of the unit cell dimers to preformed crystal [12,16,17,32,33]. Indeed, this observation may explain why quinidine is a more potent *in vitro* crystal growth inhibitor than chloroquine, despite having a lower FP affinity because quinidine may have a higher affinity for the FP crystal [24].

Despite the importance of FP crystal growth as an antimalarial drug mechanism, little is known about how the quinolines affect the kinetics of crystal growth. Recent studies of uninhibited FP crystal growth kinetics show the reaction is sigmoidal, analogous to a biomineralization processes [13,34]. This finding suggests that previous studies of FP crystal growth inhibitors, which measure inhibition at fixed reaction times, may be misleading in regards to the time dependence and potency. To study the kinetics and other characteristics of FP crystal growth, we developed a rapid spectrophotometric assay for determination of β-hematin growth. This assay is then used in a high-throughput screen for compounds that cause inhibition of crystal growth (ICG).

2. Materials and methods

2.1. FP crystal growth reaction

The FP crystal growth reaction is performed as previously described [16,20]. Briefly, 5 nmol (FP content) of preformed β-hematin is used to seed FP crystal growth with 50 μM FP substrate in 0.5 mL 0.1 M ammonium acetate, pH 4.8 at 37°. The seed β-hematin is prepared by the method of Egan in a single large batch used for all assays [13,35]. The yield was more than 20 μmol by heme content of purified β-hematin for which Fourier transform infrared spectra have been published on similar purified preparations on two separate occasions [36,37]. DMSO concentrations are below 1% in all assays. Chemicals are reagent grade and at least 99% pure. Bovine hemin chloride and the chemicals tested in the high-throughput screen are from Sigma-Aldrich. Fluconazole (Pfizer) was obtained in solution from the hospital pharmacy. Compounds used in the high-throughput screen are dissolved in water or DMSO. FP is prepared fresh daily in DMSO with an extinction coefficient $\varepsilon_{400} = 100{,}000\ M^{-1}\ cm^{-1}$. All experiments, in triplicate reactions, had absorbance values determined twice in a spectrophotometer or microplate reader to minimize pipet errors. For time-course reactions, multiple individual reactions are set up to be processed at set intervals.

2.2. Field emission inlens scanning electron microscopy (FEISEM)

Heme crystal reaction product processed by Assay-1 below except the addition of 2% SDS/50 mM NaOH was deleted and the crystal product washed with distilled water and applied to silica chip as described previously [37].

2.3. Crystal growth determination assays

Three different crystal determination assay methods are used to quantify FP crystal growth from the reaction: (Assay-1) Product from the FP crystal reaction is purified as previously described [16] (Assay-2). After solubilization of free FP in the crystal growth reaction with addition of concentrated stock solutions to obtain 0.15 M sodium bicarbonate, pH 9.1, 2% SDS in 1.5 mL, the FP crystal is pelleted by centrifugation at 18,000 *g* for 10 min. Spectrophotometric quantification of 0.1 mL of supernatant determined free FP. Addition of 0.1 mL 10 M NaOH-decrystallized the rest of the FP in the reaction tube for subsequent quantification. The amount of crystal FP is calculated using the following Eq. (1):

$$\text{FP in FP crystal (M)} = \frac{1}{\varepsilon_{400}}(A_{400}\text{NaOH} - 0.933A_{400}\text{NaHCO}_3) \quad (1)$$

A_{400}NaOH is the absorbance after decrystallization and A_{400}NaHCO$_3$ is the absorbance of monomeric FP dissolved in 0.15 M sodium bicarbonate, pH 9.1, 2% SDS in the first step. A factor of 0.933 corrects for the absorbance of the 0.1 mL removed to quantitate monomeric FP in the 0.15 M sodium bicarbonate, pH 9.1, 2% SDS step. ε_{400} is the molar extinction coefficient (Assay-3). For high-throughput FP crystal assays in 24-well microplates, growth reactions are at the same concentrations in 0.25 mL. Monomeric FP is quantified after addition of 0.5 mL of concentrated sodium bicarbonate/SDS. The correction factor changes to 0.866. This assay involves no centrifugations and no changing of plates or tubes. The assay is based on the very low absorbance of FP crystals compared to monomeric FP at 400 nm [18]. For compounds that absorbed significantly at 400 nm, measurement of FP

crystals is determined by Assay-1. IC_{50} values are calculated using four-parameter logarithmic analysis using GraphPad Prism. Data are presented ±SE of the mean of triplicate reactions.

2.4. Absorption spectra

Experiments are performed at room temperature in matched quartz cuvettes as previously described [38,39]. A 17 μM FP solution in 40% DMSO, 20 mM HEPES, pH 7.5 is prepared from a stock solution of FP in DMSO. Compounds used in the spectroscopic studies are also dissolved in 40% DMSO, 20 mM HEPES, pH 7.5. All compounds are equilibrated with the FP solutions for at least 5 min before spectra are taken. For titration experiments, a reference cuvette containing an identical FP solution is titrated with the DMSO/HEPES buffer.

2.5. Labeled ketoconazole parasite hemozoin binding experiments

Assessment of ketoconazole binding to hemozoin in cultured intraerythrocytic parasites and *in vitro* is performed as described previously [16,32]. ^{3}H-ketoconazole (American Radiolabeled Chemicals cat. no. ART-794) has a specific activity of 5 Ci/mmol. For cultured parasites, 7.14 μCi of ^{3}H-ketoconazole is added to each 10 mL plate instead of the 0.5 μCi used previously with chloroquine or quinidine [16]. For the *in vitro* binding assays 1 μCi of ^{3}H-ketoconazole is added to combinations of 10 nmol of hemozoin and 5 or 25 nmol of FP.

3. Results

3.1. Crystal growth extension

β-Hematin seed crystals were chosen because a single large *in vitro* reaction product can yield enough product after purification for uniform seeding of all of the crystal growth reactions rather than purification of the more limited parasite hemozoin. For this crystal growth reaction the equilavence of product growth and inhibition with quinolines by seeding either with hemozoin from parasites or with β-hematin has been validated [37]. The process of seeded crystal growth has also been theoretically modeled by Buller *et al.* [33]. Morphology of purified crystal growth product from seed crystals of purified *P. falciparum* hemozoin is similar to crystals grown from seed crystals of the β-hematin preparation by FEISEM (Fig. 1). Areas of rapid growth are depicted emanating at different angles from seed crystals. Although the product is morphologically different from parasite-derived hemozoin, the unit cell structure of hydrogen bonded Fe1–O41 dimers is the same.

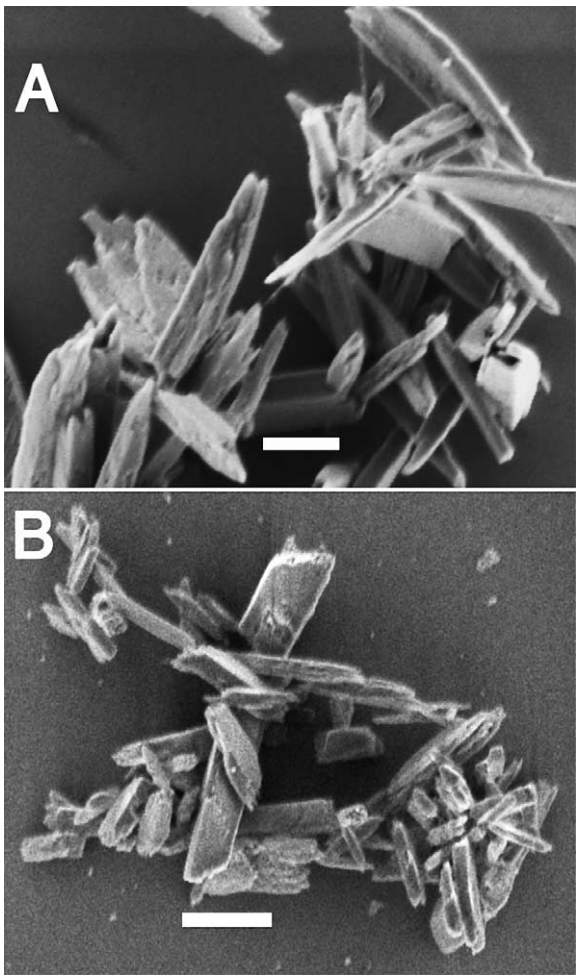

Fig. 1. FEISEM of purified crystal growth product. Seed FP crystals of parasite derived hemozoin (A) or β-hematin (B) incubated overnight with 50 μM FP substrate in 0.5 mL 0.1 M ammonium acetate, pH 4.8 at 37° were purified by Assay-1 to remove noncrystalline FP. FP crystals were deposited onto silica chips for FEISEM. The white bar equals 200 nm.

3.2. Development of a new determination assay to measure FP crystal growth

The crystal determination assays (2 and 3) presented here allow for rapid and accurate measurement of FP crystal based on both the differential solubility of free and crystalline FP in sodium bicarbonate pH 9.1 solutions and also on the large difference in absorbency of soluble free FP vs. insoluble crystalline FP at 400 nm [18,40]. If increasing amounts of β-hematin from 5 to 30 nmol are added to FP in acetate buffer, pH 4.8, and processed using the previously published Assay-1 [13] or two newer assays, the resultant standard curve of the quantification of β-hematin recovered by each method has a slope of one and the variance agrees to within a nanomolar. In these comparative experiments used to generate the standard curve, β-hematin and FP are varied in concentration such that the total FP of seed crystal plus free FP always equals 50 nmol. Assay-2 is easily adaptable to multiple, rapid kinetic experiments if a microplate reader is used. Assay-3 can

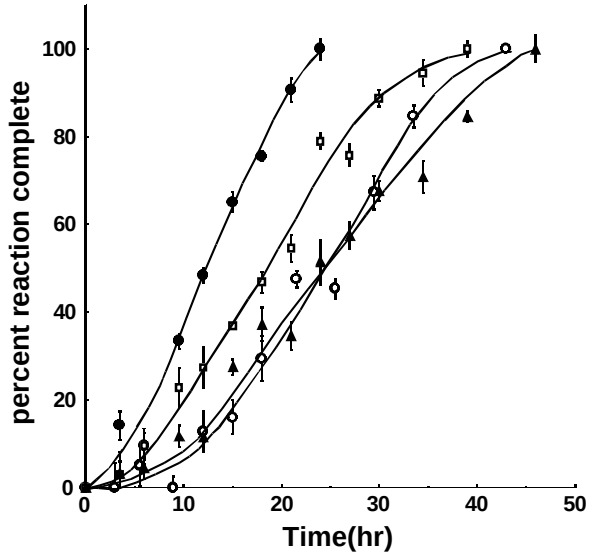

Fig. 2. ICG by chloroquine, quinidine and ketoconazole. β-Hematin, 5 nmol, and FP, 50 μM, are incubated in 0.5 mL 0.1 M ammonium acetate, pH 4.8 at 37° with no drug (●), 5 μM chloroquine (▲), 1 μM quinidine (□), and 6 μM ketoconazole (○). The amount of new β-hematin formed is measured at various times. Total amount of new FP crystal formed at final time points by FP content: control, 20.7 nmol; chloroquine, 24.1 nmol; quinidine, 23.6 nmol and ketoconazole, 20.77 nmol. SEM is for triplicate incubations.

be performed in the incubation vessel without centrifugation, making it amenable for high-throughput screening in 96-well plates. Thus, the new assays presented here are as accurate and reproducible as a previously published method [16,20]. These experiments are designed such that the amount of substrate FP added and seed crystal is within detection range of spectrophotometer.

3.3. Kinetics of FP crystal growth

FP crystal growth of a 5 nmol (FP content) β-hematin seed is measured over time at 37° using Assay-2. In the absence of inhibitor, the reaction shows sigmoidal time dependence complete by 20 hr with a 4–6 hr lag time (Fig. 2). The sigmoidal kinetics of crystal growth are similar if β-hematin or parasite-derived hemozoin seed the reaction (data not shown). This suggests that the average surface area of β-hematin crystals mimics the more regular surface area of *P. falciparum* hemozoin. At 60° the β-hematin seeded reaction is complete by 4 hr with a similar sigmoidal time dependence (data not shown). Pre-incubation of the FP substrate for 2–6 hr at 37° prior to addition of the β-hematin seed does not affect the lag time, suggesting that time-dependent changes in FP do not account for the lag time. In addition, if FP from NaOH-decrystallized β-hematin is used as a substrate, the kinetics of crystal growth are identical (data not shown). These experiments suggest that the lag phase of the crystal growth reaction is not related to onset of FP dimerization into the Fe1–O41 unit crystal and that decrystallization with NaOH is complete with no remnant Fe1–O41 dimers or larger crystals to accelerate the recrystallization. Previous studies of FP crystal growth kinetics show a significant relationship between reaction rate and stirring speed [13,34]. Shaking the FP crystal growth reaction at approximately 150 rpm on a rotary shaker at 37° has no effect on the reaction rate or shape of the curve (data not shown). However, sonication of the FP substrate solution in the acidic ammonium acetate buffer, either before or after the addition of β-hematin seed, greatly increased the rate of FP crystal growth at 37°. All the FP crystallizes by 12 hr instead of 20 hr while the sigmoid shape of the curve is preserved (data not shown). However, sonication does not increase the concentration of soluble FP, which remains at 3–5 μM. This discrepancy could possibly be explained by increased dispersion of FP with sonication, which lowers the aggregate size of insoluble FP, resulting in greater mobilization of FP from the aggregate state to soluble FP at this pH. In contrast, the use of 10% DMSO in the reaction increases product by 30% at 12 hr by increasing the amount of soluble FP. Increasing FP to 100 or 150 μM also increases the crystal yield at 12 hr by 30 and 60%, respectively. The crystal reaction presently used is likely to be less susceptible to variations in rate due to stirring than other systems which use millimolar concentrations of FP that are up to 40 times as concentrated as the 50 μM FP in these assays.

3.4. ICG by chloroquine and quinidine is reversible

Previous studies of the effects of the quinoline antimalarials on FP crystal growth report the extent of inhibition at a fixed time points, typically overnight [41–44]. Given the importance of FP crystal growth to the mechanism of quinoline drugs, kinetic analysis should yield insight on the time dependence and potency of inhibition. The FP crystal growth reaction is performed in the presence of 5 μM chloroquine and 1 μM quinidine (Fig. 2) which is near the IC_{50} concentration of a 12 hr assay (discussed below). Significantly, inhibition is reversible as the reaction proceeds to completion in approximately twice the time of the uninhibited reaction for both chloroquine and quinidine. The crystal growth reaction retains the sigmoidal time dependence, while quinidine and chloroquine appear to negatively affect both the lag time and growth phase of the reaction. Again, use of either β-hematin or hemozoin from parasites as seed crystal did not effect the drug inhibition curves. The finding that ICG by the quinolines is reversible complicates interpretation of previous work that measured inhibition at fixed time-points. Specifically, the quinolines appear less potent at longer time periods given the reversible inhibition.

The potency of ICG is studied at 12 hr of incubation at 37° because this coincides with the apparent maximum rate of the uninhibited crystal growth reaction. Under these experimental conditions, IC_{50} values are 1.5 ± 0.2 μM and

4.3 ± 0.2 μM for quinidine and chloroquine, respectively. In the case of chloroquine, the phosphate counter ion did not effect any inhibition at the highest drug concentrations tested (data not shown).

3.5. Increasing the β-hematin seed reverses inhibition of FP crystal growth

The quinoline antimalarials have been proposed to inhibit FP crystal growth by either incorporating at growth sites [16] or sequestering monomeric FP from the reaction [22]. To test these hypotheses, the FP crystal growth reaction is performed with increasing FP substrate or β-hematin seed. If the quinolines work by sequestering monomeric FP, then inhibition can be overcome by increasing the starting concentration of FP. On the other hand, if the quinolines incorporate at growth sites on the crystal, inhibition can be overcome by increasing the number of growth sites available.

FP crystal growth reactions are performed as described in the absence or presence of 13.5 μM chloroquine, 22.5 μM ketoconazole, or 4.5 μM quinidine at 12 hr. ICG is expressed as a percentage of the uninhibited reaction performed with an identical amount of FP or β-hematin seed. Increasing the amount of FP substrate in the reaction had no effect on the extent of inhibition up to the highest concentration tested of 0.2 mM (data not shown). In contrast, increasing the β-hematin seed decreased inhibition by all three inhibitors (Fig. 3). With 5 nmol (FP content) of β-hematin seed, the crystal growth reaction is inhibited by 97% for ketoconazole, 66% for chloroquine, and 74% for quinidine. With 50 nmol of β-hematin seed, there is an approximately 50% decrease in inhibition for all three drugs.

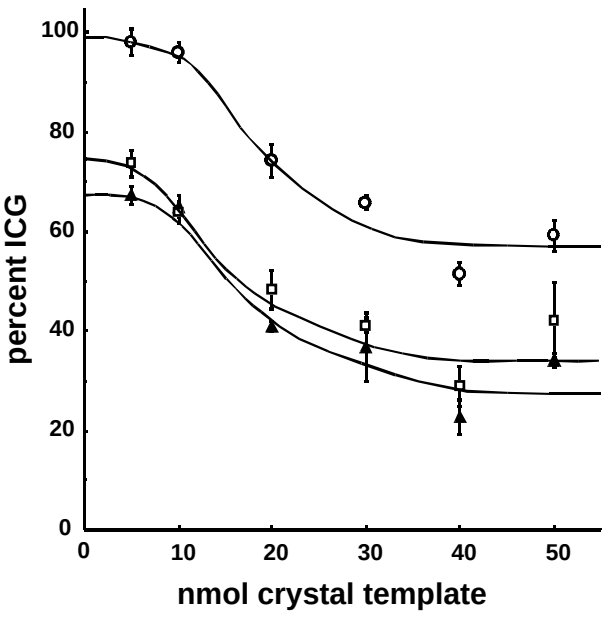

Fig. 3. Increasing amounts of β-hematin seed reverse ICG. Various amounts of β-hematin seed crystal template are incubated for 12 hr with 13.5 μM chloroquine (▲), 22.5 μM ketoconazole (○) or 4.5 μM quinidine (□), and 50 μM FP in 0.5 mL 0.1 M ammonium acetate, pH 4.8. Percent ICG is expressed as a ratio of new crystal growth with drug divided by new crystal growth with the no drug control reaction started with the same amount of β-hematin seed template.

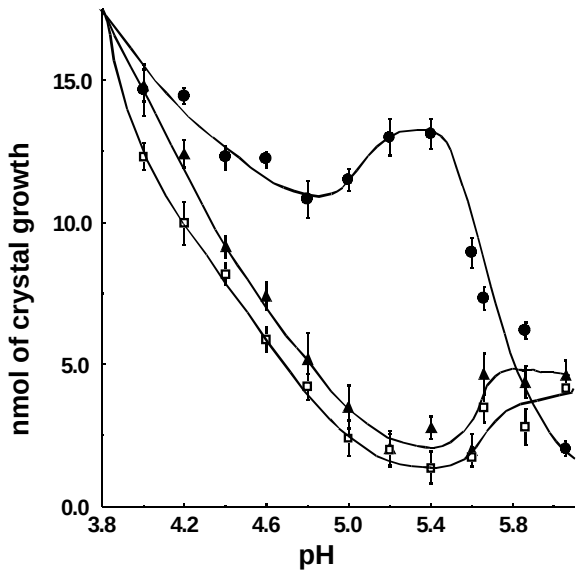

Fig. 4. pH dependence of FP crystal growth. FP crystal growth assay is performed in 0.5 mL with 50 μM FP, 5 nmol β-hematin in the absence (●) or presence of 2.25 μM quinidine (□) or 6.75 μM chloroquine (▲). Ammonium acetate, 0.1 M is used for pH 4–5.6; MES, 0.1 M is used for pH 5.66–6.0. SEM is for triplicate incubations performed with two independent experiments.

3.6. Effect of pH on FP crystal growth and quinoline ICG

For the uninhibited reaction, the amount of FP crystal growth decreases as pH increases from 4.0 to 4.8 (Fig. 4). Above pH 5.0 the amount of FP crystal formed by 12 hr increases to reach a local maxima at pH 5.3 that is nearly equivalent to the amount formed at pH 4.0. From pH 5.3 to 6.0 the amount of FP crystal formed rapidly decreases, such that the reaction is almost completely inhibited at pH 6.0. In the presence of the quinoline antimalarials chloroquine and quinidine, the extent of ICG increases with pH, to reach a maximum of nearly 100% inhibition at pH 5.4. Interestingly, both chloroquine and quinidine also demonstrate a slight local maxima increase at pH 5.8, which is 0.5 pH higher than the control local maxima.

To test whether aggregation/nucleation abrogates the effects of drugs on ICG, FP is pre-incubated at 37° in the presence or absence of 2 μM quinidine for 2 hr in 0.1 M ammonium acetate, pH 4.4, 4.8 or 5.2. The FP crystal growth reaction is then initiated by the addition of a 5 nmol β-hematin seed and incubated for 12 hr at 37°. At pH 4.4, 4.8, and 5.2 no significant difference in inhibition is observed if FP is pre-incubated in buffer followed by

the addition of quinidine or if FP is pre-incubated with quinidine.

3.7. High-throughput screening for FP crystal growth inhibitors

Assay-2 used above in kinetic and pH experiments is adapted for high-throughput screening by deleting the centrifugation step to produce Assay-3. The low absorbance of FP crystal does not interfere significantly with FP quantification after addition of bicarbonate/SDS [18]. The low ratio of starting FP crystal to free FP minimizes errors. This allows hundreds of compounds to be screened in a day. Furthermore, the method in this screen avoids radioactive chemicals, transfer of solutions to filter paper or centrifugation steps used in other high-throughput protocols [22,44–46]. A limited library of 105 compounds was pilot tested, with emphasis placed on clinically-available drugs. Inhibitors are characterized as being "strong" if $\geq$50% ICG is observed at 20 μM, "moderate" if $\geq$50% ICG is observed at 50 μM, and "no inhibition" if there is less than 50% ICG at 50 μM (Table 1).

Most antimalarials previously reported to block FP crystal growth score as "strong inhibitors," validating this high-throughput approach. These drugs include amodiaquine (IC_{50} 1.2 ± 0.2 μM), quinacrine (IC_{50} 4.9 ± 0.7 μM), and quinine (IC_{50} 17.1 ± 0.7 μM) [22,43]. This assay is further validated by the lack of ICG by antimalarials that kill the parasite by other mechanisms such as pyrimethamine and doxycycline. Primaquine, which is inactive

Table 1
High-throughput ICG screen results

Strong inhibition (>50% at 20 μM)			
Compound	ICG IC_{50} (μM) {[FP]/ICG IC_{50}}	IC_{50} CQ-susceptible parasites (strain, reference)	IC_{50} CQ-resistant parasites (strain, reference)
Classic antimalarials			
Amodiaquine	1.2 ± 0.2 {42}	7.8 nM (3D7, [43]) 8.5 nM (HB3, [43]) 3.0 nM (NF54, [47])	18.5 nM (K1, [43]) 13.8 nM (PH3, [43])
Chloroquine	4.3 ± 0.2 {12}	14.0 nM (3D7, [43]) 18.5 nM (HB3, [43]) 13.0 nM (NF54, [48]) 24.0 nM (D6, [49]) 10.0 nM (NF54, [47]) 9.5 nM (CDC1, [50])	192.0 nM (K1, [43]) 158.8 nM (PH3, [3]) 122.0 nM (W2, [49]) 140.0 nM (K1, [50])
Quinacrine	4.9 ± 0.7 {10}	8.0 nM (NF54, [47]) 9.0 nM (CDC1, [50])	3.1 nM (K1, [50])
Quinidine	1.5 ± 0.2 {33}	21.5 nM (3D7, [43]) 23.9 nM (HB3, [43])	50.6 nM (K1, [43]) 43.6 nM (PH3, [43])
Quinine	17.1 ± 0.7 {3}	34.2 nM (3D7, [43]) 36.8 nM (HB3, [43]) 22.0 nM (NF54, [22])	81.2 nM (K1, [43]) 74.3 nM (PH3, [43])
Antifungal cytochrome P450 inhibitors			
Clotrimazole	12.9 ± 0.6 {4}	431.0 nM (HB3, [51]) 245.0 nM (NF54, [51])	1.1 μM (A4, [51]) 553.0 nM (W2, [51]) 1.0 μM (ITG2, [52])
Econazole	19.7 ± 1.9 {3}	–	–
Ketoconazole	6.5 ± 0.6 {8}	~9.4 μM (Honduras I/CDC, [53,54])	~1.0 μM (Indochina I/CDC, [54])
Miconazole	21.4 ± 2.2 {2}	–	~400.0 nM (I/CDC, [54])
Antimalarial dyes[a]			
Azure A	33.7 ± 1.7 {1}	10.2 nM (D6, [49])	10.5 nM (W2, [49])
Brilliant cresyl blue	29.0 ± 0.9 {2}	9.7 nM (D6, [49])	5.5 nM (W2, [49])
Methylene blue	28.9 ± 2.3 {2}	3.6 nM (D6, [49])	4.0 nM (W2, [49])
Nile blue	1.7 ± 0.2 {30}	51.0 nM (D6, [49])	42.0 nM (W2, [49])
Other			
Amphotericin	1.7 ± 0.4 {29}	–	~400.0 nM (I/CDC, [54,55])
Bilirubin	6.6 ± 1.3 {8}	–	–
Biliverdin	0.6 ± 0.1 {91}	–	–
Biochanin A	20.8 ± 1.1 {2}	164.0 μM (poW, [56])	–
Distamycin	16.1 ± 0.5 {3}	0.7 μM (ITO4, [57])	618 nM (FCR3, [58]) 330 nM (FCR3, [59])
Ellipticine	7.9 ± 0.8 {6}	–	–
Genistein	36.2 ± 3.4 {1}	7.4 μM (poW, [56])	14.8 μM (Dd2, [56])
Zinc protoporphyrin IX	19.6 ± 0.5 {3}	No inhibition (D10, [60])	No inhibition, (Dd2, [60])

Table 1 (*Continued*)

Moderate inhibition (>50% at 50 μM)			
Compound			
Acridine orange	Artemesinin	L-Canaline	Ketotifen
Nystatin	D-Penicillamine	Pentamidine	Phloridizin
Primaquine	Rifampicin	Tamoxifen	Thionine
No inhibition at 50 μM			
Acetaminophen	Acetohydroxamic acid	AGT	Albendazole
Amantidine	Amitryptiline	Ampicillin	Aspirin
Atovaquone	Benzophenone	Berberine	Caffeine
Chlorpheniramine	Cimetidine	Cinnamic acid	Coumarin
Cyproheptadine	Deferoxamine mesylate	Dibucaine	Diphenhydramine
Disulfram	Doxycycline	Ebselen	EDTA
Efrapeptin	Ferrozine	Fluconazole	Griseofluvin
Guaifesen	Histamine	Hydralazine	Hydroxyquinoline
8-Hydroxyquinoline	5-Hydroxytryptamine (serotonin)	Hydroxyurea	Hypoxanthine
Ibuprofen	Imipramine	Indole	Isoniazid
Mebendazole	Menadione	Methimazole	Metronidazole
Metyrapone	Mianserin	Minocycline	Mizorbine
Neocuproine	Netropsin	Nifedipine	Norfloxacin
Orphenadrine	Oxibendazole	Phenanthrene	Pyrimethamine
Riboflavin	Safranin	SDS	Streptomycin
Sulfaphenazole	Sulfapyridine	Sulfasalazine	Sulfathiazole
Tetracycline	Theophylline	Thiabendazole	Tolnaftate

[a] Included for interest and not potency of inhibition.

against intraerythrocytic stages of infection is weakly associated with ICG ($IC_{50} > 50$ μM). The relevance of primaquine as an inhibitor of crystal growth is questionable given that some groups observe inhibition [45,46,61], while others do not [22,35,43].

One interesting finding of this screen is that dyes reported to have antimalarial activity also have ICG, including Azure A (IC_{50} 33.7 ± 1.7 μM), methylene blue (IC_{50} 28.9 ± 2.3 μM), and Nile blue (IC_{50} 1.7 ± 0.2 μM). Methylene blue is of historical interest because in 1891 it became the first reported synthetic rather than natural compound to clinically cure malaria, although its use was limited by side effects [44,49,62]. Other unexpected finds in the ICG screen are compounds previously reported to have antimalarial activity, including: genistein (IC_{50} 36.2 ± 3.4 μM) a kinase inhibitor; biochanin A (IC_{50} 20.8 ± 1.1 μM), an isoflavone from the bark of the medicinal plant *Andira inermis* [56]; and distamycin (IC_{50} 16.1 ± 0.5 μM), an antibiotic which binds in the minor groove of AT-rich DNA sequences. The antifungal drugs amphotericin (IC_{50} 1.74 ± 0.4 μM), which disrupts membranes and binds sterols, also demonstrated ICG. Inhibition is most likely unrelated to the detergent properties of this drug as SDS at similar concentrations did not inhibit the reaction. The FP metabolites biliverdin and bilirubin (IC_{50} 0.6 ± 0.1 μM and 6.6 ± 1.3 μM, respectively) are potent inhibitors and most likely act by forming complexes with FP. Ginsburg has proposed an accounting system to compare different crystal growth assays where the concentration of FP used in the *in vitro* assay is divided by the IC_{50} to obtain an integral ratio (Table 1) [44]. Potent inhibitors have a ratio greater than two.

Other CYP inhibitors besides quinidine showed ICG, including ellipticine (IC_{50} 7.9 ± 0.8 μM) and the azole antifungals clotrimazole (IC_{50} 12.9 ± 0.6 μM), econazole (IC_{50} 19.7 ± 1.9 μM), ketoconazole (IC_{50} 6.5 ± 0.6 μM), and miconazole (IC_{50} 21.4 ± 2.2 μM). Significantly, clotrimazole has recently been reported to inhibit chloroquine-sensitive and -resistant parasites in the micromolar range [39,51,63]. In contrast, no inhibition of FP crystal growth or inhibition of parasites in culture at concentrations as high as 100 μM is observed for fluconazole, which is disappointing given that this drug is provided free of charge by Pfizer in 50 least-developed countries.

Previous studies on the relationship between FP crystal growth inhibition and parasite growth inhibition suggest a correlation exists if factors such as the extent of drug accumulation and FP binding affinity are considered [22,30,43]. Because the reversible nature of FP crystal growth inhibition suggests previous IC_{50} values underestimate potency, we compared our values with IC_{50} data for *in vitro* culture growth inhibition of chloroquine-sensitive and -resistant parasites. In cases where several culture growth IC_{50} values are reported, an average is taken. No direct correlation is observed between the extent of ICG and growth inhibition of cultures for sensitive or resistant parasites for compounds with IC_{50} values in Table 1. Furthermore, no relationship is found for quinolines that are reported to have a direct correlation between ICG and growth inhibition (amodiaquine, chloroquine, quinacrine, and quinine) [22]. No correlation between ICG and reported drug-FP binding affinity was also seen [38,47,64,65].

3.8. Inhibition of FP crystal growth by compounds discovered in the high-throughput screen is reversible

To determine if reversible inhibition of FP crystal growth observed with quinoline antimalarials is generalized to other inhibitors, compounds discovered in the high-throughput screen are incubated at IC_{50} concentration in the standard reaction mixture. After a 48-hr incubation at 37° inhibition is observed to be reversible for all strong inhibitor compounds listed in Table 1 with the exception of zinc protoporphyrin IX, which remains completely inhibited. To further study reversible inhibition, a detailed time-course reaction is performed with ketoconazole, with concentrations near IC_{50} (Fig. 2). Like the time-course for the quinoline antimalarials, a sigmoidal curve is observed for reversible inhibition by ketoconazole. This compound affects both the lag and crystal growth phases, and inhibition is reversed by 40 hr. Based on these experiments, it appears reversible inhibition of FP crystal growth is generalized among inhibitors discovered in the high-throughput screen.

3.9. Spectra of FP–azole complexes

To study interactions between FP and the azole antifungal drugs, the absorbance spectra of 17 μM FP is recorded in 40% DMSO, 20 mM Hepes, pH 7.5.

Previous studies have shown that FP is monomeric under these conditions [38,39]. FP alone gives a characteristic absorbance spectra with a Soret band at 401 nm and Q-bands at 496 and 617 nm (Fig. 5A). Addition of 0.2 mM clotrimazole or 0.2 mM ketoconazole results in a virtually identical change in the FP absorbance spectra, with the Soret band decreased in intensity and redshifted to 407 nm and the Q-bands increased in intensity and changed to 531 nm and approximately 557 nm. This spectra is similar to those previously reported for clotrimazole–FP complexes [39]. Addition of 0.2 mM econazole or miconazole to the FP solution results in a similar change in the absorbance spectra. The Soret bands are lower in intensity and further redshifted than in the ketoconazole/clotrimazole spectra, to 416 nm for econazole and 418 nm for miconazole. The Q-bands for econazole and miconazole occur at 535 and 557 nm and are of greater intensity than clotrimazole/ketoconazole. The spectra of all the azole FP crystal growth inhibitors studied are similar to that when FP is saturated with 2.5 mM imidazole (Soret band at 407 nm, Q-bands at 532 and 557 nm), suggesting that the azoles interact with FP via an imidazole group. Fluconazole, a triazole, showed no interaction with FP and also at 100 μM concentrations did not inhibit culture of *P. falciparum* parasites.

To further study the interaction between the azoles and FP, 17 μM FP in 40% DMSO, 20 mM Hepes, pH 7.5 is titrated with increasing amounts of econazole and the resulting spectra is compared to FP titrated with buffer

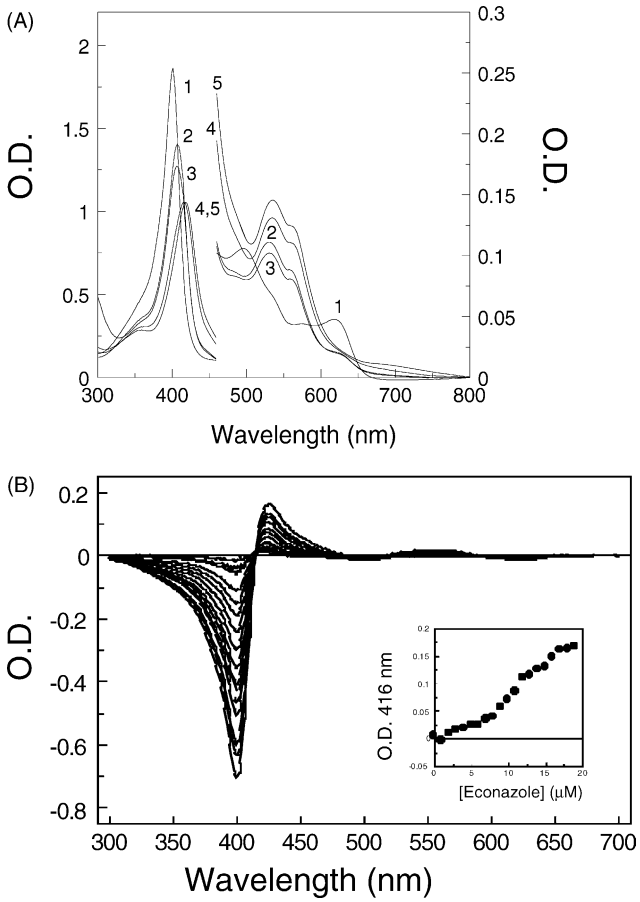

Fig. 5. Absorption spectra of FP, FP–imidazole, and FP–azole antifungal complexes. All samples are equilibrated in 20 mM Hepes, pH 7.4, 40% DMSO for 5 min, after which no further change is observed. (A) 1: 17 μM FP; 2: 2.5 mM imidazole and 17 μM FP; 3: 0.2 mM ketoconazole and 17 μM FP; 4: 0.2 mM econazole and 17 μM FP; 5: 0.2 mM miconazole and 17 μM FP. Spectra of miconazole–FP complex between 3 and 500 nm is slightly red-shifted compared to econazole–FP complex. Spectra of 0.2 mM clotrimazole and 17 μM FP, which is essentially equivalent to ketoconazole, is omitted for clarity. (B) Titration of FP with econazole. FP, 17 μM in 40% DMSO, 20 mM Hepes, pH 7.5 is titrated with 0–132 μM econazole and spectra are taken over 3–700 nm.

(Fig. 5B). As econazole concentration increases, the spectra undergoes a decrease in absorbance centered at 401, 504, and 524 nm, and shows increases centered at 426 and 562 nm, with isobestic points at 415, 491, 516 and 594 nm. These spectral changes suggest econazole forms a saturable complex with FP, and the presence of isobestic points indicates only two absorbing species are present during the titration [39].

3.10. Incorporation of ketoconazole into FP crystals

To determine whether ketoconazole reaches the proposed site of action, FP crystals in the digestive vacuole, a synchronized population of ring-stage parasites are incubated with a subinhibitory dose of 0.143 μM ^{3}H-ketoconazole until the parasites progress to trophozoite stages containing FP crystals. After cell lysis, the extent of ^{3}H incorporation into the hemozoin, purified on sucrose

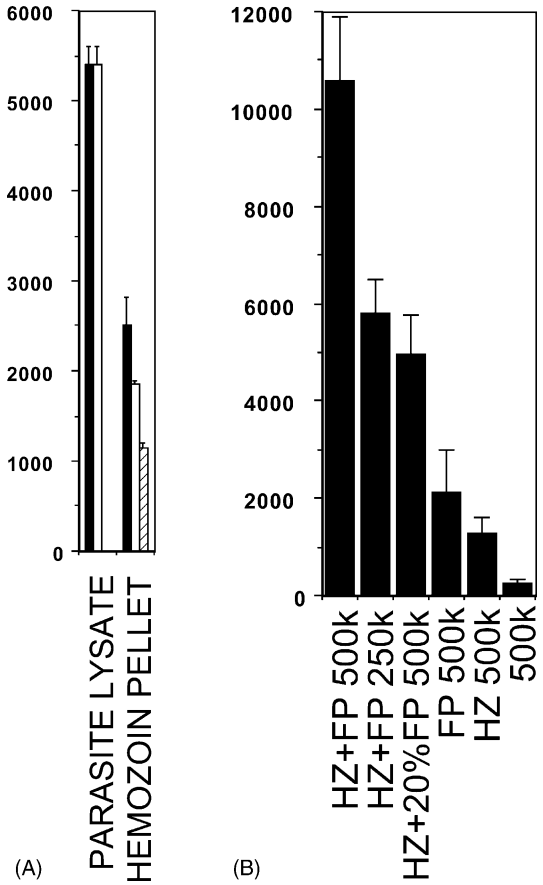

Fig. 6. ^{3}H-ketoconazole binds both to parasite hemozoin and crystal growth product. (A) Duplicate 10 mL 3D7 parasite cultures are incubated with 7.14 μCi of ^{3}H-ketoconazole, purified by hypotonic lysis and processed without (filled bars) and with (open bars) sucrose cushion ultracentrifugations. Control (striped bar) hemozoin pellet after sucrose cushion ultracentrifugation is from the same parasites grown to trophozoites in absence of drug with 7.14 μCi of ^{3}H-ketoconazole added at time of hypotonic lysis. 109,400 cpm are in these control parasite lysates before purification of hemozoin on sucrose cushions. FP content of hemozoin in ultracentrifugation pellets is 9 nmol without sucrose and 5 nmol both with sucrose and control with sucrose. (B) Overnight incubations of 10 nmol by FP content of hemozoin (HZ) and 50 μM FP or 10 μM FP (20% FP) in 100 mM sodium acetate, pH 5.0 with ^{3}H-ketoconazole, 500,000 cpm (500 k) or 250,000 cpm (250 k) are processed through sucrose cushions. Triplicate determinations of radioactivity associated with pellets are shown.

cushions, is measured (Fig. 6A). Even though 50 times the molar amount of ^{3}H-ketoconazole is used in these experiments, compared to those previously performed with ^{3}H-chloroquine [16], only a small fraction of ^{3}H-ketoconazole, 5400 cpm, associates with pelletable parasite lysates after the hypotonic lysis. A saponin lysis purification, which pellets mostly intact parasites free of erythrocyte cytosol, yields the same amount of ^{3}H-ketoconazole associated with parasites as the hypotonic lysis (data not shown). Approximately half of the 5400 cpm of ^{3}H-ketoconazole in isolated parasite fractions copurify with hemozoin on the sucrose cushions. The total accumulation with hemozoin is approximately 20% of the accumulation seen with ^{3}H-mefloquine [32]. No hemozoin copurification occurs if ^{3}H-ketoconazole is added at the time of hypotonic lysis to parasites grown to the trophozoite stage in the absence of drug. The incorporation of ^{3}H-ketoconazole into the *in vitro* crystal growth product purified on sucrose cushions is similar to the incorporation of labeled mefloquine [32] (Fig. 6B). Like the quinolines, much more ^{3}H-ketoconazole is incorporated into the crystal growth product in the presence of FP than in incubation with β-hematin alone. ^{3}H-ketoconazole alone did not pellet significantly in this assay.

4. Discussion

Many methods were developed by numerous investigators to measure FP crystal growth *in vitro*, including infrared and Mossbauer spectroscopy [34,66], radioactive [40,46], nonradioactive [44,45,61], and HPLC methods [19]. The ICG assay reported here is more rapid and convenient than previously published methods which require radioactivity, multiple centrifugation steps or filter paper washes [44,46,61]. When adapted for high-throughput screening, hundreds and potentially thousands of compounds can be screened for ICG in a day. Unlike many of the radioactive high-throughput assays, which essentially measure FP binding to up to 1000-fold excess of preformed hemozoin or β-hematin template [22,43], the current assay uses just five times as much substrate to template concentrations. This assay also uses considerably less DMSO (<1%) compared to another assay (25–50%) [44] which is significant given that prolonged incubations in 100% DMSO partially solubilizes FP crystals [15]. The lower DMSO used here is more likely to mimic soluble FP concentrations in the parasite food vacuole, given that only 5 μM FP is soluble in aqueous solutions. In addition, the lower micromolar FP concentrations used here do not require stirring and should minimize any artifacts of mixing which may be seen in assays that use millimolar concentrations of FP [35,45,61]. This assay can be adapted to 96-well by adjusting downward the millimolar concentration of the acid solution for 200 uL aqueous reaction and by adding more concentrated bicarbonate/SDS solutions in 50 uL.

These kinetic studies highlight an additional reversible component to inhibition of FP crystal formation by the quinolines and other antimalarial compounds that interact with FP. A chemical explanation for the reversible ICG is the reversible association of drug/FP complex on growth sites rather than a pure FP–substrate interaction that would not change over time. For example, increasing the amount of crystal seed, but not FP substrate, decreases inhibition by chloroquine, quinidine, and ketoconazole at a set time-point. The increasing amounts of crystal seed in this experiment is analogous to later time-points in kinetic experiments. Once a certain number of crystal growth sites exceeds the drug/FP incorporation, crystal growth proceeds. At later time-points, the drug/FP complex disassociates

from a growth site, such that an Fe1–O41 dimer is able to incorporate into the crystal at a site of drug/FP disassociation. Compounds with a low FP binding affinity may be potent inhibitors because they dissociate very slowly from the FP crystal once bound. In as much as chloroquine and quinidine have similar potency at ICG, while quinine is over 10 times less potent, suggests an additional heme crystal inhibition step to just FP binding affinity [24,31]. Furthermore, performing inhibition when the crystal growth reaction proceeds at a maximal rate (i.e. 12 hr vs. "overnight") gives IC_{50} values that are between 3- and 15-fold more potent than previously described for chloroquine: $IC_{50} = 80$ μM, overnight incubation [46]; $IC_{50} = 24.4$ μM, overnight incubation [43]; $IC_{50} = 15$ μM [30] or quinidine, $IC_{50} = 24$ μM, overnight [43].

The local maxima increase in FP crystal formation at pH 5.3 complements the reported steep increase in FP solubility with an increase in pH reported by Roepe and coworkers [67]. They account for the steep rise in solubility because of the diprotic weak acid of the two propionic carboxylic acids of FP have a pK_a near pH 5.5. Other pH titrations of FP crystal formation, which note a decrease in crystal formation as pH increases, were performed with increments of 0.5 pH units or greater, and may have missed the local maxima seen in this work [68,69]. Another previous pH titration by Dorn *et al.* was, in effect, an FP binding experiment as 14 nmol of FP was incubated with 10,000–20,000 nmol of seed crystal β-hematin [47], whereas our crystal growth assay uses 25 nmol of FP and 5 nmol of seed crystal β-hematin. This large difference in assay conditions may explain why the pH maxima based on increased solubility of FP near the pK_a of the side chain carboxylate groups was not seen before. Interestingly, the shift in local maxima from pH 5.3 to 5.8 that occurs in the presence of chloroquine and quinidine, corresponds to the reported shift in the midpoint of the FP pH-dependent solubility curve reported by the Roepe group [67].

The drugs screened in this study for ICG included the nitrogen heterocycles ellipticine and the azole antifungal drugs, which inhibit CYP demethylation of lanosterol in fungi. Many CYP inhibitors bind FP in the active site. Quinine and quinidine have been known to inhibit CYP enzymes for decades [70]. *P. falciparum*, *P. yoelii*, and *P. knowlesi* all possess a CYP reductase homologue, however a putative CYP homologue has not been identified yet in the *P. falciparum* genome [71]. Although putative CYP transcripts were identified by Northern Blot analysis using a rat gene as a probe [72] and enzymatic activity was seen after an assay [73], the existence of substantial CYP activity in the intraerythrocytic stages remains in question. In the early 1980s, ketoconazole and miconazole were reported to inhibit *in vitro* parasite culture in the micromolar range, which is near the peak concentrations ranging from 1 to 10 μM obtained in humans upon oral administration [53]. Recently, this observation was extended to clotrimazole [51,52]. Although the azole antifungals have been shown to protect FP from glutathione degradation [39], recent data argue that more than 90% of FP released by hemoglobin degradation remains in the digestive vacuole as hemozoin [7]. Controversy continues about the mechanism of action of the quinolines like chloroquine or the antifungal azoles like clotrimazole acting on heme crystal growth, glutathione degradation of heme or possibly CYP activity [17,74].

Egan has proposed a hierarchy of inhibition of *Plasmodium* parasites by drugs that bind FP: not all drugs that bind FP inhibit *in vitro* FP crystal formation. Not all drugs that bind FP and inhibit FP crystal formation localize to the target site in the digestive vacuole [64]. This data clearly show that many of the CYP inhibitors that bind FP are potent at ICG. However, only a slight amount of ^{3}H-ketoconazole copurifies with hemozoin from parasites cultured with subinhibitory concentrations and with FP crystals generated in the *in vitro* seeding reaction. The lesser extent of accumulation compared to chloroquine or quinidine may be an artifact of the purification assay, which involves multiple centrifugations and washes. During the 2-hr sucrose cushion purification, ketoconazole could dissociate more than chloroquine or quinidine. Further studies to localize the other azoles to the food vacuole will help in determining the extent to which ICG accounts for their antimalarial activity.

The triazole, fluconazole, did not appreciably bind FP, inhibit crystal growth, or block *P. falciparum* parasites *in vitro*. Triazoles inhibit CYP51 through coordination of N-4 in the triazole ring with the heme iron of the cytochrome. In addition, hydrophobic interactions between the N-1 substituent and the apoprotein of the active site have also been proposed as being important in determining the affinity of fluconazole for the enzyme. Co-crystal growth of the *Mycobacterium* CYP51 with fluconazole shows that apoprotein contacts are as important as the N-4 FP contacts [75]. Despite type II spectral changes in fluconazole binding heme of CYP, we did not observe direct spectral changes with heme alone. The lack of *P. falciparum* inhibition is disappointing given the reduced hepatotoxicity of fluconazole compared to ketoconazole, and the fact that fluconazole is freely distributed in developing countries to treat HIV-candidiasis. Nevertheless, the abundance of FDA-approved drugs that inhibit CYP by binding FP opens the possibility that currently approved medicines may be of interest in developing new antimalarial treatments. Such antimalarials may hinder the development of resistance by attacking the parasite in multiple ways, such as blocking FP crystal growth, inhibiting potential CYP enzymes, and interfering with other FP-sensitive pathways.

Acknowledgments

D.J.S. received financial assistance from the Burroughs Wellcome Career Award in Biomedical Sciences, Pew

Scholars Program in Biomedical Sciences and NIH RO1 AI45774-01. An NCCR Grant GPDGCRC RR0052 supports the use of RBC for culturing *P. falciparum*. The authors thank Lirong Shi for assistance with *Plasmodium* culture. C.R.C. gratefully acknowledges the encouragement of Drs. Patrick, Patricia, and Joao Okinedo.

References

[1] Wellems TE, Plowe CV. Chloroquine-resistant malaria. J Infect Dis 2001;184:770–6.
[2] Sturchler D. How much malaria is there worldwide? Parasitol Today 1989;5:39–40.
[3] WHO, Malaria Fact Sheet No. 94. http://www.who.int/inf-fs/en/fact094.html 1998.
[4] Macreadie I, Ginsburg H, Sirawaraporn W, Tilley L. Antimalarial drug development and new targets. Parasitol Today 2000;16:438–44.
[5] Olliaro PL, Yuthavong Y. An overview of chemotherapeutic targets for antimalarial drug discovery. Pharmacol Ther 1999;81:91–110.
[6] Winstanley P. Modern chemotherapeutic options for malaria. Lancet Infect Dis 2001;1:242–50.
[7] Egan TJ, Combrinck JM, Egan J, Hearne GR, Marques HM, Ntenteni S, Sewell BT, Smith PJ, Taylor D, Van Schalkwyk DA, Walden JC. Fate of haem iron in the malaria parasite *Plasmodium falciparum*. Biochem J 2002;365:343–7.
[8] Krugliak M, Zhang J, Ginsburg H. Intraerythrocytic *Plasmodium falciparum* utilizes only a fraction of the amino acids derived from the digestion of host cell cytosol for the biosynthesis of its proteins. Mol Biochem Parasitol 2002;119:249–56.
[9] Gluzman IY, Francis SE, Oksman A, Smith CE, Duffin KL, Goldberg DE. Order and specificity of the *Plasmodium falciparum* hemoglobin degradation pathway. J Clin Invest 1994;93:1602–8.
[10] Orjih AU, Banyal HS, Chelvi R, Fitch CD. Hemin lyses malarial parasites. Science 1981;214:667–9.
[11] Pagola S, Stephens PW, Bohle DS, Kosar AD, Madsen SK. The structure of malaria pigment beta-hematin. Nature 2000;404:307–10.
[12] Bohle DS, Kosar AD, Madsen SK. Propionic acid side chain hydrogen bonding in the malaria pigment beta-hematin. Biochem Biophys Res Commun 2002;294:132–5.
[13] Egan TJ. Physico-chemical aspects of hemozoin (malaria pigment) structure and formation. J Inorg Biochem 2002;91:19–26.
[14] Bohle DS, Helms JB. Synthesis of β-hematin by dehydrohalogenation of hemin. Biochem Biophys Res Commun 1993;193:504–8.
[15] Slater AF, Swiggard WJ, Orton BR, Flitter WD, Goldberg DE, Cerami A, Henderson GB. An iron-carboxylate bond links the heme units of malaria pigment. Proc Natl Acad Sci USA 1991;88:325–9.
[16] Sullivan Jr DJ, Gluzman IY, Russell DG, Goldberg DE. On the molecular mechanism of chloroquine's antimalarial action. Proc Natl Acad Sci USA 1996;93:11865–70.
[17] Sullivan D. Hemozoin: a biocrystal synthesized during the degradation of hemoglobin. In: Matsumura S, Steinbüchel A, editors. Miscellaneous biopolymers, biodegradation of synthetic polymers, vol. 9. Germany, Weinheim: Wiley-VCH, Verlag GmbH & Co.; 2002. p. 129–163; In: Steinbuchel A, editor. Biopolymers.
[18] Fitch C, Cai G, Chen Y, Shoemaker J. Involvement of lipids in ferriprotoporphyrin IX polymerization in malaria. Biochim Biophys Acta 1999;1454:31–7.
[19] Bendrat K, Berger BJ, Cerami A. Haem polymerization in malaria. Nature 1995;378:138.
[20] Goldberg DE, Sharma V, Oksman A, Gluzman IY, Wellems TE, Piwnica-Worms D. Probing the chloroquine resistance locus of *Plasmodium falciparum* with a novel class of multidentate metal(III) coordination complexes. J Biol Chem 1997;272:6567–72.
[21] Dorn A, Stoffel R, Matile H, Bubendorf A, Ridley RG. Malarial haemozoin/betahaematin supports haem polymerization in the absence of protein. Nature 1995;374:269–71.
[22] Dorn A, Vippagunta SR, Matile H, Bubendorf A, Vennerstrom JL, Ridley RG. A comparison and analysis of several ways to promote haematin (haem) polymerisation and an assessment of its initiation *in vitro*. Biochem Pharmacol 1998;55:737–47.
[23] Slater AF, Cerami A. Inhibition by chloroquine of a novel haem polymerase enzyme activity in malaria trophozoites. Nature 1992;355:167–9.
[24] Slater AF. Chloroquine: mechanism of drug action and resistance in *Plasmodium falciparum*. Pharmacol Ther 1993;57:203–35.
[25] Homewood CA, Jewsbury JM, Chance ML. The pigment formed during haemoglobin digestion by malarial and schistosomal parasites. Comp Biochem Physiol 1972;43B:517–23.
[26] Yayon A, Cabantchik ZI, Ginsburg H. Susceptibility of human malaria parasites to chloroquine is pH dependent. Proc Natl Acad Sci USA 1985;82:2784–8.
[27] Cohen SN, Phifer KO, Yeilding KL. Complex formation between chloroquine and ferrihaemic acid *in vitro*, and its effect on the antimalarial action of chloroquine. Nature 1964;202:805–6.
[28] Chou AC, Chevli R, Fitch CD. Ferriprotoporphyrin IX fulfills the criteria for identification as the chloroquine receptor of malaria parasites. Biochemistry 1980;19:1543–9.
[29] Moreau S, Perly B, Chachaty C, Deleuze C. A nuclear magnetic resonance study of the interactions of antimalarial drugs with porphyrins. Biochem Biophys Acta 1985;840:107–16.
[30] Vippagunta SR, Dorn A, Matile H, Bhattacharjee AK, Karle JM, Ellis WY, Ridley RG, Vennerstrom JL. Structural specificity of chloroquine–hematin binding related to inhibition of hematin polymerization and parasite growth. J Med Chem 1999;42:4630–9.
[31] Leed A, DuBay K, Ursos LM, Sears D, De Dios AC, Roepe PD. Solution structures of antimalarial drug–heme complexes. Biochemistry 2002;41:10245–55.
[32] Sullivan Jr DJ, Matile H, Ridley RG, Goldberg DE. A common mechanism for blockade of heme polymerization by antimalarial quinolines. J Biol Chem 1998;273:31103–7.
[33] Buller R, Peterson ML, Almarsson O, Leiserowitz L. Quinoline binding site on malaria pigment crystal: a rational pathway for antimalaria drug design. Cryst Growth Des 2002;2:553–62.
[34] Egan TJ, Mavuso WW, Ncokazi KK. The mechanism of beta-hematin formation in acetate solution. Parallels between hemozoin formation and biomineralization processes. Biochemistry 2001;40:204–13.
[35] Egan T, Ross D, Adams P. Quinoline anti-malarial drugs inhibit spontaneous formation of beta-haematin (malaria pigment). FEBS Lett 1994;352:54–7.
[36] Sullivan DJ, Gluzman IY, Goldberg DE. *Plasmodium* hemozoin formation mediated by histidine-rich proteins. Science 1996;271:219–22.
[37] Chen MM, Shi L, Sullivan DJ. *Haemoproteus* and *Schistosoma* synthesize heme polymers similar to *Plasmodium* hemozoin and β-hematin. Mol Biochem Parasitol 2001;113:1–8.
[38] Egan TJ, Mavuso WW, Ross DC, Marques HM. Thermodynamic factors controlling the interaction of quinoline antimalarial drugs with ferriprotoporphyrin IX. J Inorg Biochem 1997;68:137–45.
[39] Huy NT, Kamei K, Yamamoto T, Kondo Y, Kanaori K, Takano R, Tajima K, Hara S. Clotrimazole binds to heme and enhances heme-dependent hemolysis: proposed antimalarial mechanism of clotrimazole. J Biol Chem 2002;277:4152–8.
[40] Slater AFG, Cerami A. Inhibition by chloroquine of a novel haem polymerase enzyme activity in malaria trophozoites. Nature 1992;355:167–9.
[41] Baelmans R, Deharo E, Munoz V, Sauvain M, Ginsburg H. Experimental conditions for testing the inhibitory activity of chloroquine on the formation of β-hematin. Exp Parasitol 2000;96:243–8.
[42] Cole KA, Zeigler J, Evans CA, Wright DW. Metalloporphyrins inhibit β-hematin (hemozoin) formation. J Inorg Biochem 2000;78:109–15.

[43] Hawley SR, Bray PG, Mungthin M, Atkinson JD, O'Neill PM, Ward SA. Relationship between antimalarial drug activity, accumulation, and inhibition of heme polymerization in *Plasmodium falciparum in vitro*. Antimicrob Agents Chemother 1998;42:682–6.

[44] Deharo E, Garcia RN, Oporto P, Gimenez A, Sauvain M, Jullian V, Ginsburg H. A nonradiolabelled ferriprotoporphyrin IX biomineralisation inhibition test for the high throughput screening of antimalarial compounds. Exp Parasitol 2002;100:252–6.

[45] Basilico N, Pagani E, Monti D, Olliaro P, Taramelli D. A microtitre-based method for measuring the haem polymerization inhibitory activity (HPIA) of antimalarial drugs. J Antimicrob Chemother 1998;42:55–60.

[46] Kurosawa Y, Dorn A, Kitsuji-Shirane M, Shimada H, Satoh T, Matile H, Hofheinz W, Masciadri R, Kansy M, Ridley RG. Hematin polymerization assay as a high-throughput screen for identification of new antimalarial pharmacophores. Antimicrob Agents Chemother 2000; 44:2638–44.

[47] Dorn A, Vippagunta SR, Matile H, Jaquet C, Vennerstrom JL, Ridley RG. An assessment of drug–haematin binding as a mechanism for inhibition of haematin polymerisation by quinoline antimalarials. Biochem Pharmacol 1998;55:727–36.

[48] Vippagunta SR, Dorn A, Bubendorf A, Ridley RG, Vennerstrom JL. Deferoxamine: stimulation of hematin polymerization and antagonism of its inhibition by chloroquine. Biochem Pharmacol 1999;58: 817–24.

[49] Vennerstrom JL, Makler MT, Angerhofer CK, Williams JA. Antimalarial dyes revisited: xanthenes, azines, oxazines and thiazines. Antimicrob Agents Chemother 1995;39:2671–7.

[50] Webster RV, Craig JC, Shyamala V, Kirby GC, Warhurst DC. Antimalarial activity of optical isomers of quinacrine dihydrochloride against chloroquine-sensitive and resistant *Plasmodium falciparum in vitro*. Biochem Pharmocol 1991;42:S225–7.

[51] Tiffert T, Ginsburg H, Krugliak M, Elford BC, Lew VL. Potent antimalarial activity of clotrimazole in in vitro cultures of *Plasmodium falciparum*. Proc Natl Acad Sci USA 2000;97:331–6.

[52] Saliba KJ, Kirk K. Clotrimazole inhibits the growth of *Plasmodium falciparum in vitro*. Trans R Soc Trop Med Hyg 1998;92:666–7.

[53] Pfaller MA, Krogstad DJ. Imidazole and polyene activity against chloroquine-resistant *Plasmodium falciparum*. J Infect Dis 1981; 144:372–5.

[54] Pfaller MA, Krogstad DJ. Oxygen enhances the antimalarial activity of the imidazoles. Am J Trop Med Hyg 1983;32:660–5.

[55] McColm AA, McHardy N. Evaluation of a range of antimicrobial agents against the parasitic protozoa, *Plasmodium falciparum*, *Babesia rodhaini* and *Theileria parva in vitro*. Ann Trop Med Parasitol 1984;78:345–54.

[56] Kraft C, Jenett-Siems K, Siems K, Gupta MP, Bienzle U, Eich E. Antiplasmodial activity of isoflavones from *Andira inermis*. J Ethnopharmacol 2000;73:131–5.

[57] Lombardi P, Crisanti A. Antimalarial activity of synthetic analogues of distamycin. Pharmacol Ther 1997;76:125–33.

[58] Ginsburg H, Nissani E, Krugliak M, Williamson DH. Selective toxicity to malaria parasites by non-intercalating DNA-binding ligands. Mol Biochem Parasitol 1993;58:7–15.

[59] Lee S, Inselburg J. In vitro sensitivity of *Plasmodium falciparum* to drugs that bind DNA or inhibit its synthesis. J Parasitol 1993;79: 780–2.

[60] Martiney JA, Cerami A, Slater AF. Inhibition of hemozoin formation in *Plasmodium falciparum* trophozoite extracts by heme analogs: possible implication in the resistance to malaria conferred by the beta-thalassemia trait. Mol Med 1996;2:236–46.

[61] Parapini S, Basilico N, Pasini E, Egan TJ, Olliaro P, Taramelli D, Monti D. Standardization of the physicochemical parameters to assess in vitro the beta-hematin inhibitory activity of antimalarial drugs. Exp Parasitol 2000;96:249–56.

[62] Guttmann P, Ehrlich P. Uber die wirkung des methylenblau bei malaria. Berliner Klinische Wochenschrift 1891;39:953–6.

[63] Saliba KJ, Folb PI, Smith PJ. Role for the *Plasmodium falciparum* digestive vacuole in chloroquine resistance. Biochem Pharmacol 1998;56:313–20.

[64] Egan JT, Hunter R, Kaschula HC, Marques MH, Misplon A, Walden J. Structure–function relationships in aminoquinolines: effect of amino and chloro groups on quinoline–hematin complex formation, inhibition of B-hematin formation, and antiplasmodial activity. J Med Chem 2000;43:283–91.

[65] Fitch CD, Kanjananggulpan P. The state of ferriprotoporphyrin IX in malaria pigment. J Biol Chem 1987;262:15552–5.

[66] Adams PA, Egan TJ, Ross DC, Silver J, Marsh PJ. The chemical mechanism of beta haematin formation studied by Mossbauer spectroscopy. Biochem J 1996;318(Pt 1):25–7.

[67] Ursos LM, DuBay KF, Roepe PD. Antimalarial drugs influence the pH dependent solubility of heme via apparent nucleation phenomena. Mol Biochem Parasitol 2001;112:11–7.

[68] Lynn A, Chandra S, Malhotra P, Chauhan SV. Heme binding and polymerization by *Plasmodium falciparum* histidine rich protein II: influence of pH on activity and conformation. FEBS 1999;459:267–71.

[69] Blauer G, Akkawi M. Investigations of B- and β-hematin. J Inorg Chem 1997;66:145–52.

[70] Otton SV, Kalow W, Seeman P. High affinity of quinidine for a stereoselective microsomal binding site as determined by a radioreceptor assay. Experientia 1984;40:973–4.

[71] Gardner MJ, Hall N, Fung E, White O, Berriman M, Hyman RW, Carlton JM, Pain A, Nelson KE, Bowman S, Paulsen IT, James K, Eisen JA, Rutherford K, Salzberg SL, Craig A, Kyes S, Chan MS, Nene V, Shallom SJ, Suh B, Peterson J, Angiuoli S, Pertea M, Allen J, Selengut J, Haft D, Mather MW, Vaidya AB, Martin DM, Fairlamb AH, Fraunholz MJ, Roos DS, Ralph SA, McFadden GI, Cummings LM, Subramanian GM, Mungall C, Venter JC, Carucci DJ, Hoffman SL, Newbold C, Davis RW, Fraser CM, Barrell B. Genome sequence of the human malaria parasite *Plasmodium falciparum*. Nature 2002;419:498–511.

[72] Surolia N, Karthikeyan G, Padmanaban G. Involvement of cytochrome P-450 in conferring chloroquine resistance to the malarial parasite, *Plasmodium falciparum*. Biochem Biophys Res Commun 1993;197:562–9.

[73] Ndifor AM, Ward SA, Howells RE. Cytochrome P-450 activity in malarial parasites and its possible relationship to chloroquine resistance. Mol Biochem Parasitol 1990;41:251–7.

[74] Sullivan DJ. Theories on malarial pigment formation and quinoline action. Int J Parasitol 2002;32:1645–53.

[75] Podust LM, Poulos TL, Waterman MR. Crystal structure of cytochrome P450 14alpha—sterol demethylase (CYP51) from *Mycobacterium tuberculosis* in complex with azole inhibitors. Proc Natl Acad Sci USA 2001;98:3068–73.